Cryst. Growth & Des. 10 (2010) 691–699 Magnetic Field

DATASET · MAY 2013

5 AUTHORS, INCLUDING:

Abel Moreno
Universidad Nacional Autónoma de México
81 PUBLICATIONS **969** CITATIONS

DOI: 10.1021/cg901109e

CRYSTAL GROWTH & DESIGN Article

2010, Vol. 10 691–699

Investigations into Protein Crystallization in the Presence of a Strong Magnetic Field

Sachin Surade,[†] Takashi Ochi,[†] Daniel Nietlispach,[†] Dima Chirgadze,[†] and Abel Moreno*[,†,‡]

[†]*Department of Biochemistry, University of Cambridge, 80 Tennis Court Road CB2 1GA Cambridge, U.K. and* [‡]*Instituto de Química, Universidad Nacional Autónoma de México, Circuito Exterior, C.U. México, D.F. 04510, Mexico*

Received September 10, 2009; Revised Manuscript Received December 14, 2009

ABSTRACT: A new strategy is proposed for batch crystallization of proteins in solution-growth or gel-growth by using the batch method inside capillary tubes applying magnetic fields. Four proteins with differing proportions of α-helices and β-sheets and crystallized in five different crystallographic space groups are studied, allowing an analysis of the anisotropy of the diamagnetic susceptibility of the peptide bond as well as the polarity of the space groups in the presence of a strong magnetic field of 11.75 T. The crystal quality is shown to be improved by using a strong magnetic field to orient protein molecules, and gel-growth (high concentrations of agar) to control the transport phenomena as well as crystal growth. Some advantages to increase the crystal quality for crystals from marginal conditions for X-ray diffraction, and disadvantages of the use of solution- and gel-growth (low concentration of agar) in magnetic fields, and their plausible applications to high resolution X-ray crystallography are discussed.

1. Introduction

One of the inconveniences in obtaining high quality crystals is the natural convection that exists in every experiment performed under normal Earth gravity conditions. In addition to the problems in protein crystallization arising from solutions to transport phenomena and methods of crystal growth are the number of parameters that play an important role during the crystallization process. Thus, crystallization of proteins is difficult because of our lack of understanding of many of the physicochemical properties either of protein crystals or precipitating agent solutions.[1]

Transport processes, and in particular mass transport, are very important for crystal growth from aqueous solutions.[2−4] Mass and heat transport processes are critical to the final quality and characteristics of the crystals.[5] Many crystallogenesis techniques have been explicitly developed for controlling the relative contributions of convective and diffusive transport in crystal growth.[6] During the active incorporation of ions or molecules in the three-dimensional lattice, density differences are generated in the proximal area of the developing faces leading to a convective flux in the surroundings of the crystal.[7−9] Convective transport of molecules competes with pure diffusive transport, and the sum of these two processes will determine the nature and the kinetics of nutrient presentation to the growing crystal. Transport phenomena not only affect the access of nutrients to the crystals but also the rates of adsorption and incorporation of impurities that affect their size, morphology development, and perfection.[10] On the other hand, convective transport occurs only in the presence of a gravity field. Only then can heavier fluids go down and lighter fluids go up, allowing convective currents to emerge in the bulk of the solution. Other types of convection do exist, like the convection due to surface tension,[11] but they are not significant in the crystallization process of solutions. Convection should play an important role when temperature differences happen inside the sample.

It is possible to reduce natural convection on Earth with the help of magnetic fields, depending on whether they are homogeneous or inhomogeneous, as they act upon a sample in different ways. Inhomogeneous magnetic fields (in the *c*-axis direction of the crystallographic structure) are responsible for reducing the effective gravity that a solution feels. This appears to have a cumulative effect.[12] If a magnetic field gradient is applied vertically, a magnetic force will be generated. When this force opposes gravitational field, a reduction of vertical acceleration (effective gravity) is obtained. Hence, a decrease in natural convection can be accomplished.

A mathematical model of the crystallization system under a magnetic field allows the estimation of the concentrations of macromolecules in the surroundings of a growing crystal.[13] Interestingly, the high-resolution of high-quality crystals obtained experimentally were in good agreement with the mathematical model.[14]

When a homogeneous magnetic field is applied, high quality crystals are also observed,[15] even though the mechanism involved is different. An increase in viscosity near the growing crystal was observed when a magnetic field of 10 T was applied,[16,17] leading to a reduction of natural convection inside the solution. Furthermore, an orientation effect was observed upon the crystals formed under high magnetic fields.[12] More recently, the diminution of the diffusion coefficient of lysozyme inside a crystallization solution under a homogeneous magnetic field of 6 and 10 T was evaluated.[18] All these observations are interrelated and they are the consequence of the orientation effect by the magnetic field at a microscopic level. In a supersaturated solution, proteinaceous nuclei are suspended in the solution bulk, and they sediment upon reaching an adequate size depending on the magnitude of the magnetic field applied. These nuclei act as blocks avoiding the free diffusion of monomers, making the solution more viscous and, as a result, having less convection.[18] However, the research field of crystal growth under magnetic

*To whom correspondence should be addressed. E-mail: carcamo@unam.mx.

Published on Web 12/23/2009

Table 1. Crystallization Conditions for All Proteins Studied in This Experiment

protein	lysozyme	lysozyme	thaumatin	ferritin	INHA-NAD[a]
(mg/mL)	(Sigma Cod. L-6876) (tetragonal)	(Sigma Cod. L-6876) (monoclinic)	(Sigma Cod. T-7638) (tetragonal)	(Sigma Cod. F-4503) (cubic)	(wild-type) (hexagonal)
(stock solutions)	120 mg/mL in 0.1 M	40 mg/mL in 0.1 M	75 mg/mL in 0.1 M	30 mg/mL in 0.1 M	10 mg/mL
	Na acetate pH 4.6	Na acetate pH 4.6	phosphate pH 7.0	Na citrate pH 5.6	INHA was incubated for 1 h with NADH (final 1 mM)
precipitant (stock solutions)	NaCl	$NaNO_3$	KNa tartrate	$CdSO_4$	MPD
	120 mg/mL in 0.1 M	0.6 M in 0.1 M	45% (w/v) in 0.1 M buffer	80 mM, ammonium sulfate 1.0 M in 0.1 M	6−12% v/v in buffer
	Na acetate pH 4.6	Na acetate pH 4.6	phosphate pH 7.0	Na-citrate pH 5.6	Na citrate 50 mM (pH 6.5), HEPES (100 mM pH 7)
agar (stock solutions)	0.21% and 0.60% w/v	0.60% w/v	0.21% w/v and 0.60% w/v	0.21% w/v	0.21% w/v

[a] INHA-NAD is a wild-type of InhA-encoded 2-trans enoyl-acyl carrier protein reductase enzyme (InhA) from *Mycobacterium tuberculosis* in complex with NADH (reduced form of nicotinamide adenine dinucleotide).

fields is relatively new and needs more study. Fundamental aspects of the effects of magnetic fields over macromolecular crystals and macromolecular solutions remain to be understood. An external, strong magnetic field not only induces a magnetizing force but also increases the viscosity of the protein solution, orients the growing crystals, and affects the growing process in a complex manner.[16,17] All these phenomena seem to favor the resulting crystal quality, although a more complete investigation is needed to understand the mechanism better.

It is worth mentioning that the use of strong magnetic fields is still very expensive if performed only in crystallization experiments. Maintenance of the superconductive magnets and the magnet itself is expensive and consequently, an important limiting factor. However, there are recent publications that have demonstrated that application of only a 2.4 T magnetic field coupled with growth-in-gels improves the diffraction resolution limit as well as the crystal quality.[19] The combined effects of a magnetic field and magnetic field gradients on convection in crystal growth also have been published elsewhere.[20] More recently, novel experiments, using a popular magnet commonly used for nuclear magnetic resonance (NMR) used in chemistry laboratories, demonstrated different configurations for batch crystallization and gel-growth.[21,22] In spite of the results already published, there are some facts that are still not clear and deserve special attention. Some questions arise such as, is the gel (or low concentration agar) necessary to grow crystals inside magnetic fields? Is the polarity of the space group or the crystallographic system important for this orientation, and crystal quality enhancement? Is the α-helix content important given the anisotropy of the diamagnetic susceptibility of the peptide bond? Additionally, there is a lack of data about the magnetic fields applied for different proteins. Most of the data already published deal with lysozyme as the model protein, which have been important to understand the fundamentals of the methods proposed. So far, few efforts have been made to investigate different proteins at the same time.[23,24]

In this contribution, we analyze the combination of the crystal growth method in capillary tubes by using the batch-method (solution and gel) and applying a strong magnetic field of 11.75 T (corresponding to 500 MHz, 1H frequency) in NMR tubes. We tested four proteins having five different crystallographic space groups as well as different α-helices and β-sheets content. The importance of the polarity of the space group was also evaluated in detail for a monoclinic system. This was done because of the preferential polar growth in terms of crystal morphology of this space group $P2_1$ for a monoclinic lysozyme. A significant effect was noticed on the orientation of the crystals after 48 h in the presence of a strong magnetic field of 11.75 T. The crystal quality from different crystallographic systems was investigated using solution-growth and gel-growth in a strong magnetic field of 11.75 T. The gel-growth (using viscous non-Newtonian solutions of agar) used to grow and to improve the transport properties of protein crystals was further investigated. However, gel-growth using agar at low concentration did not show any substantial improvement in the crystal quality compared to the solution-growth in a strong magnetic field. The crystal quality was improved at higher concentrations of agar (0.2% w/v) in the presence of this strong magnetic field of 11.75 T.

2. Experimental Section

2.1. Protein Concentration. All concentrations were measured in triplicate by means of a spectrophotometer NanoDrop ND-1000 (BCM Houston Texas, USA) following the calibration procedures from the supplier. A calibration concentration plot was obtained for each protein, before and after crystallization aliquots of 3 μL were measured in triplicate when necessary.

2.2. Protein Crystallization. In all cases, the protein was mixed 1:1:1 (e.g., 5 μL + 5 μL + 5 μL) in the following order: precipitant, agar (0.21 or 0.60%), and protein (Table 1). In the cases of solution, the gel was replaced by water to preserve the same crystallization conditions as in the gel-growth. All protein crystals were grown in solution and in gel media by the batch method. In our case, 15-μL droplets were set up in an Eppendorf tube by mixing 5 μL of the protein stock solution with 5 μL of precipitating solution and 5 μL of 0.21% or 0.60% (w/v) stock agar gel solution (prepared in water). For the batch method, all concentrations were reduced by 1/3. Once mixed, the solution or the gelled-mix was introduced into disposable calibrated pipettes of 50 μL (Sigma-Aldrich Cod. Z-543292 of 1.0-mm inner diameter) by means of capillarity forces or sucking the capillary tube helped by using a plastic latex tubing. Green mounting clay from Hampton research (Cod. HR4-326) was used to seal both ends of the capillary tubes.

The capillary pipettes were then transferred to NMR tubes and left for 48 h under the presence of a magnetic field of 11.75 T. After finishing the experiment, the capillary pipettes were extracted from the NMR tube, cut and both sides open using a glass-capillary cutting stone (Hampton Research Cod. HR4-334). Once the ends of the capillary are opened, a little air pressure (by using plastic latex tubing) was sufficient to extrude the solution or gel with the crystals in a drop of mother liquor or cryoprotectant on a two-wells glass plate. When necessary, the gel was dissected with microtools; a small incision opened the gel and liberated the crystal to permit the cryoprotectant to get in and to replace the water molecules inside

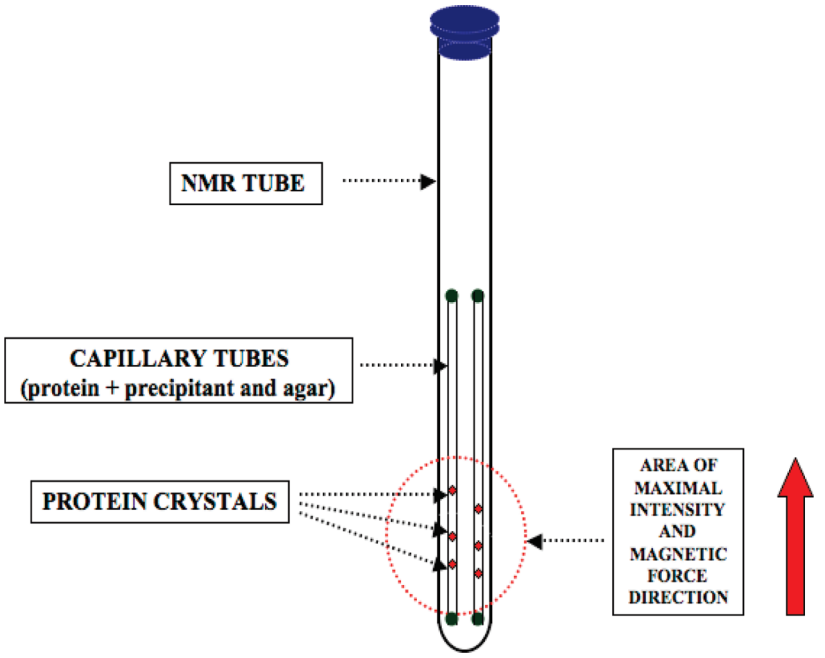

Figure 1. Experimental set up to grow protein crystals in a NMR magnet of 11.75 T (500 MHz).

Table 2. Secondary Structure Content of the Model Proteins Thaumatin and Ferritin and the Recombinant Protein INHA-NAD

protein (Space group)	thaumatin ($P4_12_12$)	ferritin ($F432$)	INHA-NAD ($P6_222$)
secondary structure composition	helical 12% beta-sheet 36%	helical 73%	helical 46% beta-sheet 15%

the structure. All crystals were immediately mounted and flash-cooled for X-ray data collection.

2.3. Gel Preparation. Agar gel 0.6% and 0.21% (w/v) stock solutions of low melting point agarose (T_{gel} = 297−298 K, Triana Sci. & Tech, Spain) were initially dissolved at 363 K, and passed through a 0.22 μm porosity membrane to remove dust or insoluble particles and were divided into 1 ml aliquots. Prior to crystallization the agarose was heated to 363−373 K and kept at 293−303 K, this allowed it to be mixed with the protein and precipitant for the classical batch method. Two concentrations of agar were tested in these experiments: agar 0.07% (w/v) and agar 0.2% (w/v) as final concentration in the mixtures.

2.4. Crystallization under the Influence of a Strong Magnetic Field. For magnetic field investigations, equal volumes of precipitating agent, gel, and protein solution were used and introduced in a capillary tube. Once sealed, the capillary pipettes were introduced into an NMR glass tube (8 mm in diameter) and then positioned in the homogeneous region of an 11.75 T magnet (Bruker NMR 500 MHz). All experiments were performed at 291 K using the temperature control unit of the NMR probe head. The tubes with the capillary pipettes were located in the region of maximum field homogeneity; as defined by the manufacturer of the NMR spectrometer (Figure 1). The sample was left in the magnetic field of 11.75 T for two or seven days as long as the crystal growth took place. The NMR tube was recovered with all capillary tubes containing several crystals along their length. The crystals were separated and flash-cooled immediately and the concentration of the mother liquor was measured when necessary.

2.5. X-ray Data Diffraction and Data Processing. Diffraction measurements were performed on beamline ID14-4 (wavelength 0.9790 Å), European Synchrotron Radiation Facility (Grenoble, France). For each protein 180 degrees of data were collected using an ADSC Q315 X-ray detector. Additional synchrotron X-ray data were also collected on beamline I03 (wavelength 0.9801 Å), Diamond Light Source (Didcot, UK), and on beamline PXIII (wavelength 0.9801 Å) at Swiss Light Source (SLS, Switzerland) for replica experiments. Two data sets of crystals grown in solution and in gel were collected for each protein and analyzed with DENZO and SCALEPACK.[25]

3. Results and Discussion

The appropriate way to look at the physical or chemical behavior of macromolecular solutions must be by means of the solubility plot of the variation of protein solubility versus the variation of the crystallization factor (concentration of precipitating agent, pH, or temperature). A typical solubility curve shows different areas of the phase diagram, where different types of phase separations take place. It has been shown that the influence of electric and magnetic fields modifies the solubility of biological systems in solution.[26] The gradient concentration generated around these fields has been demonstrated to play an important role in the homogeneous size distribution of crystals, which is closely related to the protein solubility properties.[20,27] There are different ways of investigating the solubility behavior of biomacromolecular solutions.[28,29] One is by evaluating the solubility of the protein molecules versus temperature or pH variations.[30] Additionally, we must also consider that by understanding the nucleation step based on solubility, as well as the thermodynamics and kinetics of the process, will we be able to grow high quality single crystals.

3.1. Effects of α-Helix Content and Low Agar Concentration. Selected proteins having a different secondary structure content are shown in Table 2. From the experimental results shown in Table 3, the presence of a diluted agar in a concentration around 0.07% (w/v), which behaves as a non-Newtonian liquid,[22] does not produce any substantial difference in crystal quality enhancement. It seems from the X-ray data, in general, that all crystals grown in solution (in batch) in the presence of a strong magnetic field of 11.75 T were slightly better than those grown in agar at low concentration in terms of crystal quality analysis (see the statistics

Table 3. Crystallographic X-ray Data Statistics for Ferritin Crystals (F432, rich in α-helix), Thaumatin ($P4_12_12$, Poor in α-Helix Contents)

	ferritin solution (control)	ferritin solution (magnetic)	ferritin in agar (0.07%) (magnetic)	thaumatin solution (control)	thaumatin solution (magnetic)	thaumatin in agar (0.07%) (magnetic)
unit cell, $a = b = c$ (Å)	182.42	182.28	182.65	57.92, 150.19	57.77, 150.27	57.92, 150.21
resolution range (Å)	50−2.0 (2.05−2.0)	50−1.9 (1.94−1.90)	50−2.4 (2.46−2.40)	50−1.25 (1.28−1.25)	50−1.20 (1.23−1.20)	50−1.35 (1.38−1.35)
R_{symm} (%)	7.5 (57.9)	6.1 (46.2)	9.8 (62.4)	4.8 (44.4)	5.4 (42.2)	5.7 (47.0)
completeness (%)	99.7 (100)	99.6 (100)	99.5 (100)	82 (75.1)	99.4 (98.7)	99.8 (99.7)
unique reflections	18108	20917	10711	59505	80299	57186
average redundancy	11.4	15.2	15.3	5.6	8.7	8.7
average intensity, $< I/\sigma(I) >$	12.0	15.1	9.3	12.3	11.6	11.9
% reflections with $< I/\sigma(I) > > 3^a$	48.1	54.8	50.5	60.9	57.1	58.4
Wilson B-factor (Å^2)	25.7	23.4	34.2	10.0	9.4	11.2
mosaicity (degrees)	0.58	0.53	0.68	0.35	0.29	0.28

[a] Statistics for the highest resolution shell.

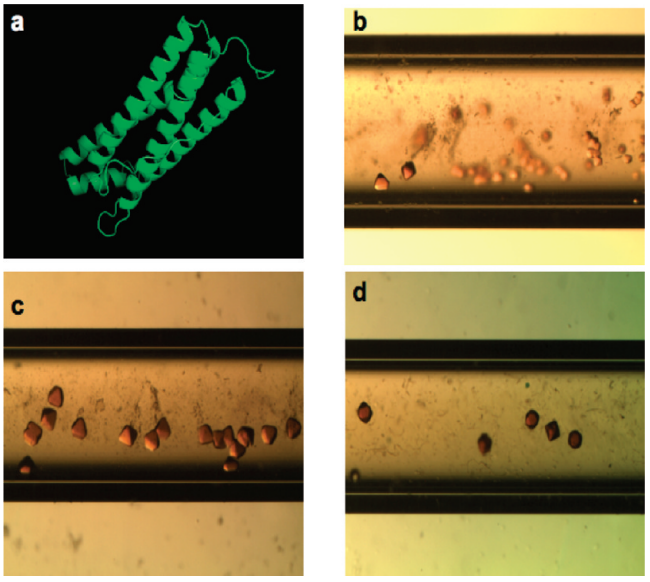

Figure 2. Crystals of ferritin grown in the presence of a strong magnetic field of 11.75 T, (a) Ferritin PDB: pdblier (b) control: in solution, (c) solution in magnetic field, and (d) gel-growth (agar 0.07% w/v) in magnetic field. As a reference for the size of all crystals, the capillary tube is 1 mm in diameter.

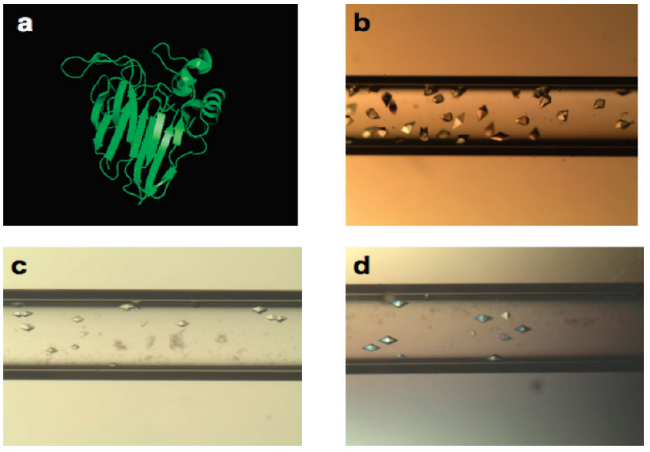

Figure 3. Crystals of thaumatin grown in the presence of a strong magnetic field of 11.75 T, (a) thaumatin PDB: 2Vl3 (b) control in solution, (c) solution in magnetic field, and (d) gel-grown (agar 0.07% w/v) in magnetic field. As a reference of the size of all crystals, the capillary tube is 1 mm in diameter.

data included in Table 3). These crystals grown in solution and in the presence of the strong magnetic field show less disorder (as indicated by the Wilson B-factor of the diffraction data, which should be low in value for high resolution crystals) and decreased values in mosaicity (which are related to the angular spread of each reflection). However, the statistical analysis of crystal quality should be taken as an overall result, and not only been assigned to one factor, like mosaicity or Wilson B-factor. On the other hand, the values of maximum resolution limit can be used as the quantitative factor of data quality.

Figures 2 and 3 show that ferritin and thaumatin crystals grown in diluted agar and in magnetic field have a more homogeneous size distribution. The solution-growth in magnetic field produced oriented crystals for thaumatin and not for ferritin, but it was observed that a few crystals were attached to each other as shown for ferritin and thaumatin (Figures 2c and 3c, respectively). In terms of anisotropy of the diamagnetic susceptibility, ferritin should be perfectly oriented because of its high α-helix content. However, this effect is counter-balanced by the symmetry of the cubic system (*F*432) and the gel fibers (viscous non-Newtonian liquid), which produces an isotropic effect in the three crystallographic directions. It is possible that for ferritin crystals this symmetry condition is causing the decrease in the crystal quality (shown in Table 3) in the presence of this strong magnetic field.

In order to test the effect of the magnetic field on the crystal quality as well as the α-helix content and low concentration agar, we analyzed crystals of the protein INHA-NAD, which have a hexagonal space group $P6_222$. In this case, the crystals grown in diluted agar did not show any substantial improvement in size (Figure 4), but they were almost perfectly oriented (either in solution or in agar at low concentration) along their *c*-axis when grown in the magnetic field (Figure 4c,d). The protein INHA-NAD was particularly interesting to work with due to its intermediate α-helix content between thaumatin and ferritin (see Table 1) and the chemical properties of the precipitating agent (MPD) used for its crystallization. Besides this efficient crystal orientation, we did not find any substantial differences in crystal quality in solution-growth or gel-growth in the magnetic field (results not shown). This is probably because the MPD used as precipitating agent may affect the polymerization properties of agar (due to the dielectric constant of the former), though most of the crystals were perfectly oriented

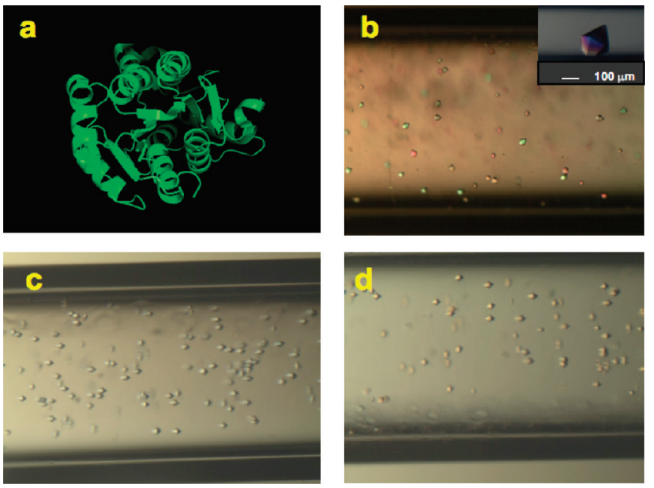

Figure 4. INHA-NAD crystals grown in a strong magnetic field of 11.75 T, (a) INHA-INH 3D-structure: INHA-NAD PDB file 2AQ8, (b) control (randomly oriented crystals): in-capillary tube, the inset shows a close up of the INHA-NAD crystal shape, (c) solution-growth of INHA-NAD in magnetic field, and (d) gel-growth (agar 0.07% w/v) of INHA-NAD in magnetic field. The size of the capillary tube is 1 mm in the inner diameter (b, c, and d).

due to the anisotropy of the diamagnetic susceptibility produced by the α-helices.

The particular property of agar at low concentration (0.07% w/v) in magnetic field to homogenize the size-distribution of oriented crystals is a potential application for studying ligand-protein on X-ray crystallographic data.

3.2. High Concentration of Agar versus Crystal Orientation. In order to test the effect of highly concentrated gel-growth in magnetic field, lysozyme and thaumatin crystals were grown in the presence of a strong magnetic field of 11.75 T for seven days, but using a higher concentration of agar 0.2% (w/v), which behaves as a classic gel in terms of its mechanical properties.[22] These crystals were bigger in size compared to those obtained in solution; however, the orientation effect was not so efficient because of the strength of the agar at this concentration. This crystal growth behavior is evident from the control experiments, solution-growth, and gel-growth of lysozyme shown in Figure 5 for lysozyme and Figure 6 for thaumatin.

Gavira and García-Ruiz have pointed out that agar at a concentration below the critical value ($C_\alpha \approx 0.12\%$ w/v) cannot be considered as a gel but rather as a viscous non-Newtonian liquid.[22] This is consistent with our results when growing lysozyme crystals in agar at higher concentrations (0.2% w/v); however, at this point we can confirm that agar in a very low concentration (below 0.12% w/v) would not be necessary at all to grow crystals under the influence of a magnetic field. Agar at low concentration is only necessary to homogenize the crystal size-distribution and to avoid the adhesion of crystals in the capillary walls. For each crystal two data sets were taken; the crystal quality trend in general was the same, but the most representative data are included in Table 4; these crystals of lysozyme grown in high concentration of agar and strong magnetic field for seven days show less disorder (as indicated by low values of the Wilson B-factor, lower values in mosaicity, and better resolution limits). However, it is very difficult to specify to what extent the quality enhancement is due to the magnetic field or to the gel itself. Recent analyses of average mosaicity of tetragonal

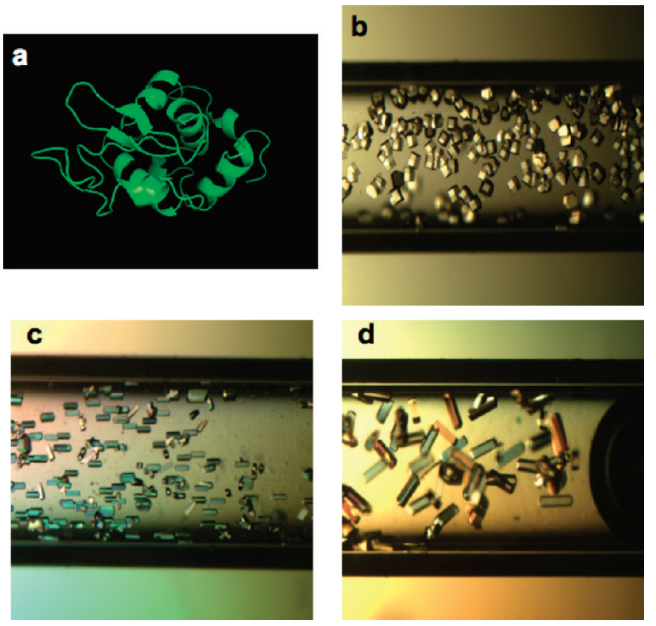

Figure 5. Crystal of lysozyme grown in the presence of a strong magnetic field of 11.75 T, (a) lysozyme PDB: l93L (b) control in solution, (c) solution in magnetic field, and (d) gel-grown (agar 0.2% w/v) in magnetic field. As a reference of the size of all crystals, the capillary tube is 1 mm in diameter.

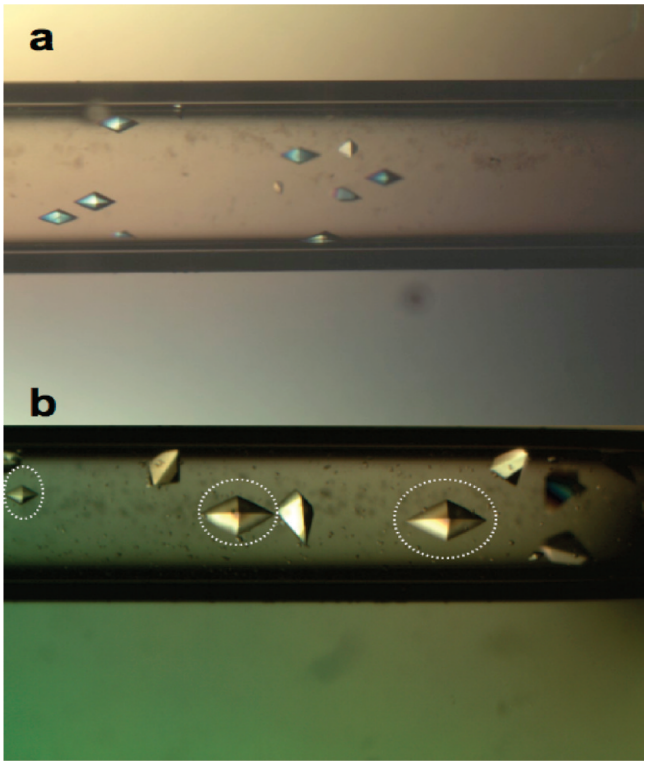

Figure 6. Thaumatin crystals grown in a strong magnetic field of 11.75 T at two concentrations of agar: (a) 0.07% and (b) 0.2% w/v. The three dotted circles show the oriented crystals along their *c*-axis in the direction of the magnetic field. As a reference of the crystal size, the capillary tube is 1 mm in diameter in both cases.

lysozyme crystals grown in 0.2% agar under a high magnetic field and characterized with X-ray topography have demonstrated the only reflections for which a tendency was observed to be improved were the crystal faces (101).[31]

Table 4. Crystallographic X-ray Data Statistics for Lysozyme Crystals (Space Group: $P4_32_12$) and Thaumatin (Space Group: $P4_12_12$) Grown in Solution and in Highly Concentrated Agar in a Strong Magnetic Field of 11.75 T

	lysozyme solution (magnetic)	lysozyme agar (0.2%) (magnetic)	thaumatin in agar (0.07%) (magnetic)	thaumatin agar (0.2%) (magnetic)
unit cell, $a = b$, c (Å)	78.58, 36.89	79.04, 36.99	57.92, 150.21	57.68, 149.63
resolution range (Å)	50−1.2 (1.23−1.20)	50−1.20 (1.23−1.20)	50−1.35 (1.38−1.35)	100−1.30 (1.33−1.30)
R_{symm} (%)	4.2 (20.1)	4.6 (17.8)	5.7 (47.0)	7.5 (45.5)
completeness (%)	99.2 (100)	99.0 (100)	99.8 (99.7)	91.2 (95.9)
unique reflections	36418	36814	57186	57927
average redundancy	8.7	8.4	8.7	6.6
average intensity, $< I/\sigma(I) >$	17.0	15.6	11.9	9.3
% reflections with $< I/\sigma(I) > > 3^a$	75.4	77.5	58.4	51.1
Wilson B-factor (Å^2)	9.7	8.6	11.2	10.2
mosaicity (degrees)	0.29	0.14	0.28	0.24

[a] Statistics for the highest resolution shell.

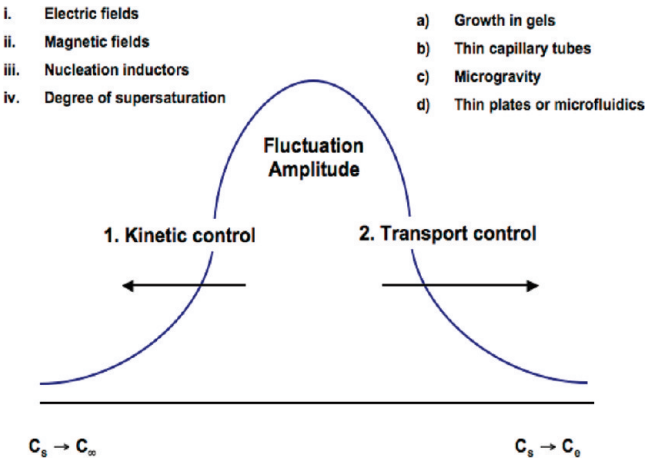

Figure 7. Rate versus transport control or kinetic control of the crystal growth process (adapted from Vekilov et al.).[32] The right-side of the figure shows different methods for increasing the crystal quality by transport control, while the left-side lists some of the approaches that can influence or affect the kinetics of the process (see the text for further explanation).

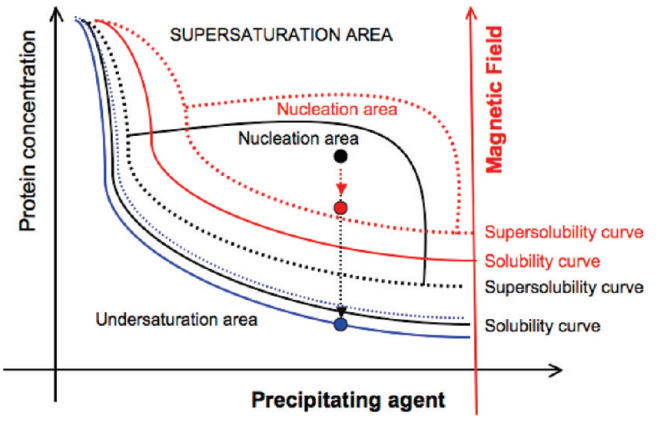

Figure 8. Conceptual protein solubility plots of batch crystallization under different experimental conditions. The black line represents the control solubility curve, the red line is the solubility curve in the presence of the magnetic field, and the blue line is the resultant curve after the experiment. The black, red, and blue spots represent the fixed crystallization conditions (protein concentration and precipitating agent ratio) for batch crystallization at the beginning, under the strong magnetic field influence, and at the end of the experiment, respectively.

As it is observed in Table 4, the same effect was obtained when agar at higher concentration (0.2%) was used for the crystallization of thaumatin for seven days in the presence of this strong magnetic field. Figure 6 shows this crystal growth behavior for thaumatin, and the same crystal quality trend for this protein is observed in Table 4 as that obtained for lysozyme, to obtain better crystals the higher the agar concentration (combined with the strong magnetic field), the higher the crystal quality is. Not all thaumatin crystals were perfectly oriented, although they were bigger in size. However, we should be aware that the higher the concentration of agar the greater the possibility of producing extra nucleation and many tiny crystals.[22]

It is clear that the rate fluctuation amplitude should be reduced in order to obtain higher quality crystals by coupling the transport and interface processes. The crystallization can proceed under pure kinetic or transport control when the interfacial solute concentration C_s approaches the bulk or equilibrium concentration (C_∞ or C_e) as shown in Figure 7.

In order to explain this crystal growth behavior in the presence of a strong magnetic field, Figure 8 shows conceptual plots, where protein aggregation behavior can be divided into the different areas where crystal growth takes place in the presence of a strong magnetic field. In the area located under the equilibrium curve (solubility curve), the protein molecules are freely distributed in the solvent, and therefore, many biomolecules are needed to saturate the system. In the upper part of this equilibrium curve (supersolubility curve), there is a parallel line where a quasi-steady state is obtained, in which there are nuclei forming and dissolving at the same time; this area is called the metastable zone. There are two forces participating in this process: the surface forces and the volume forces. In the nucleation area, the upper area above the metastable zone, where the crystal growth process takes place, nucleation occurs at high supersaturation in this area, whereas crystals growth occurs at lower supersaturation values. However, at very high supersaturation (outside this nucleation area), the system is highly supersaturated and protein−protein interactions will occur at high velocity, yielding an amorphous precipitation. The driving-force is the degree of supersaturation, related to the differences in the chemical potential of the sample and connected to the Gibbs free energy.

Transport processes can be manipulated by using different strategies. Here the convective transport is minimized by a strictly diffusive or a purely kinetic control. Figures 7 and 8 can be connected at this stage with all the crystal growth behavior observed for these proteins. The strong magnetic field affects the solubility as well as the kinetics of the process. The shape of lysozyme crystals grown in solution and gel with and without magnetic fields is consistent with

Table 5. List of Proteins and Crystallographic Space Groups Classified in Terms of Their Polarity

protein	lysozyme	lysozyme	thaumatin	ferritin	INHA-NAD
space group	$P4_32_12$	$P2_1$	$P4_12_12$	$F432$	$P6_222$
polarity: (+) polar (−) nonpolar	−	+	−	−	−

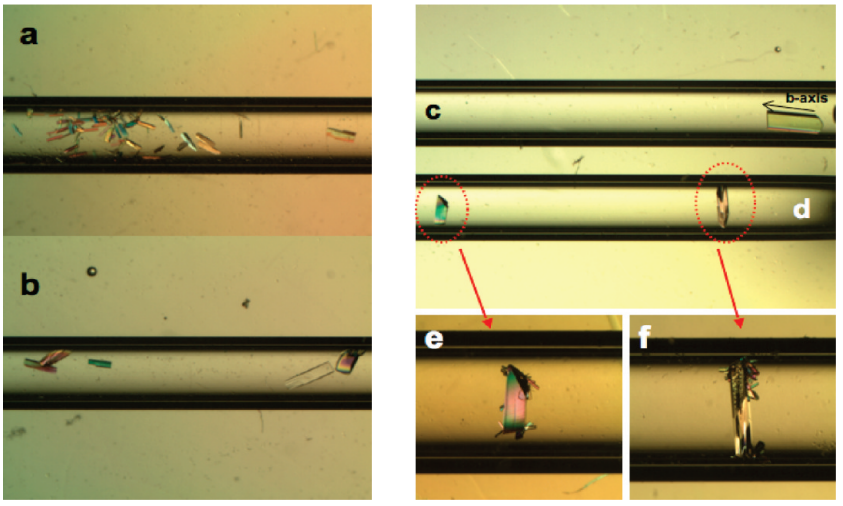

Figure 9. The capillary tube shows (a) the monoclinic lysozyme crystals ($P2_1$) grown in solution, (b) monoclinic crystals grown in solution and in magnetic field after 96 h out of the magnetic field, (c) monoclinic crystal grown in agar 0.2% (w/v). The lower capillary tube (d) shows the different shape of the monoclinic lysozyme crystals grown in agar (0.2% w/v) inside a magnetic field of 11.75 T for 2 days. As the figure shows, two crystals appear properly oriented. After 96 h out of the magnetic field, the same crystals grown in gel from Figure 9d are shown (insets e and f), but some satellite crystals (having a monoclinic shape) were starting to form in both crystals.

the solubility changes. The most elongated crystals of lysozyme are usually obtained in lower supersaturation values, while isometric-faceted crystals are usually obtained at higher supersaturation values. The conceptual plot shown in Figure 8 for batch crystallization explains why these crystals are nucleated at high supersaturation when preparing the experiment in batch. However, inside the magnetic field this supersaturation value is reduced producing growth of crystals, and it is moving the supersaturation producing a different morphology (elongated tetragonal crystals) for this lysozyme. The different types of orientation shown in experiments with lysozyme (Figure 5c,d) and thaumatin (Figure 6a,b) support this assumption and demonstrate the influence of agar concentration upon crystal quality, crystal size, and crystal orientation.

This crystal growth behavior was observed when lysozyme was grown in solution (control) showing the classic tetragonal round-shaped (isometric) with faces (110) and (101) growing almost at the same velocity, or elongated crystals observed in solution-growth and gel-growth (high concentration of agar) in magnetic field. Figure 5 shows the result of lysozyme crystals obtained under the influence of a strong magnetic field of 11.75 T versus those grown in solution. Figure 5b (control) shows the typical morphology of tetragonal lysozyme grown at high supersaturation, Figure 5c,d shows the elongated morphology of lysozyme crystals, which seems to support the assumption the magnetic field affects the supersaturation and solubility curve of the protein. The changes in the morphology of lysozyme crystals according to the degree of supersaturation and growth rates values on different crystal faces have been reported previously.[33,34] Perhaps, this crystal growth behavior, in terms of supersaturation variations, observed for lysozyme explains why two new proteins failed to crystallize using the same procedure (batch in solution and in gel). These proteins did not crystallize inside the magnetic field during two days (where crystals usually were obtained overnight in normal conditions), but after a few days out of the magnetic field these crystals started to appear and began to grow normally. The solubility changes really affected this crystallization process, yielding a kind of lag-time in the induction for this nucleation and moving the solubility plot and as a consequence the supersaturation values as conceptually described in Figure 8.

3.3. Polarity of Space Group versus Crystal Orientation. In order to test the influence of the magnetic field on the polarity of the space group as well as its influence on the crystal orientation, we selected four proteins having four nonpolar space groups (tetragonal lysozyme, tetragonal thaumatin, cubic ferritin, hexagonal INHA-NAD) and one protein monoclinic lysozyme showing a polar space group. Table 5 shows these crystallographic space groups for these studied proteins classified as polar and nonpolar. All space groups with a 2-fold axis perpendicular to the screw axis are not polar.

Monoclinic lysozyme crystals of space-group $P2_1$ were specially chosen for these experiments of crystal growth inside a strong magnetic field because of its polar crystallographic space group and the presence of a polar growth *b*-axis. The monoclinic crystals were obtained with sodium nitrate as precipitating agent, high concentrated agar (0.2% w/v), and a low concentration of lysozyme at acidic pH. However, under these crystallization conditions sometimes a triclinic form can also be obtained.[35] Figure 9 shows this crystallization behavior for control-crystals and solution-grown and gel-grown (agar 0.2% w/v) crystals in a strong magnetic field. In solution-growth, both systems produced the monoclinic phase and perhaps some triclinic crystals (Figure 9a,b), whereas the gel-growth allows nucleation and growth of only the monoclinic crystals (Figure 9c). Crystals grown in gel inside the magnetic field

(Figure 9d) were preferentially oriented, whereas in the control crystal in gel (Figure 9c) there was not a preferential orientation.

This crystal growth behavior is interesting because crystals of the monoclinic phase grow only after a few days when growing in solution, and overnight when growing in gel. The crystal growth in solution in the presence of the magnetic field presented the same behavior, but many monoclinic crystals appeared afterward. The gel-growth triggers the production of the typical monoclinic phase only (Figure 9c) with cell parameters: $a = 27.40$ Å, $b = 62.41$ Å, $c = 59.26$ Å, $\beta = 90.79$, and space group $P2_1$. On the other hand the gel-growth in magnetic field triggers a different shape of monoclinic crystals (as shown in Figures 9d) with cell parameters: $a = 27.42$ Å, $b = 62.33$ Å, $c = 59.24$ Å, $\beta = 90.89$ space-group $P2_1$. However, when stopping the magnetic field, the conditions for crystal growth were re-established, yielding satellite crystals (heterogeneous nucleation) due to high supersaturation conditions. Figure 9e,f shows this crystal growth behavior 96 h after removing the capillary from the magnetic field. It is observed that the monoclinic lysozyme gel-growth (agar 0.2% w/v) without magnetic influence was stable (used as control), but the same gel-growth experiment influenced by the magnetic field of 11.75 T was affected in some way producing satellite monoclinic crystals, which appeared afterward out of the magnetic field.

The monoclinic lysozyme crystal (space group $P2_1$) with point group 2, only the side face pairs (h 0 l) and $\bar{h}$ 0 $\bar{l}$ are related by symmetry. From the crystal growth point of view, the top faces (0 1 0) and (0 $\bar{1}$ 0) are different, which leads to the observed polar growth along the b-axis. The origin of the polar growth using the macro-bond concept as introduced by Hondoh et al.,[36] and Matsuura et al.,[37] may be found in the interactions of the crystal surface either with the solvent, or with the lysozyme molecules in the solvent. In fact, the presence of water or ions (NO_3^-) is necessary to form a crystalline contact between molecules. However, the solvent molecules can change the surface charge distribution by binding the lysozyme molecule, and as such, change the characteristics of the crystal surface. As a consequence, for polar growth to occur, the molecular structure of the opposite (h k l) and (h $\bar{k}$ $\bar{l}$) surfaces must differ as described by Heijna et al.[35] Obtaining a different shape of lysozyme monoclinic crystals in gels under the influence of the magnetic field is the result of variations in supersaturation values along the crystal growth process (Figure 9d). This effect plays an important role in the polar growth of lysozyme in the presence of this magnetic field. The changes observed in the crystal morphology as those shown in Figured 9d are probably the result of the polarity of the space group $P2_1$ as well as the existence of polar growth along the b-axis as described by the macro-bond concept.[36]

The excess of nucleation observed in Figure 9e,f, after removing the sample away from the magnetic field, is partially the result of a local higher supersaturation as the crystal does not grow and so it does not lower the solute concentration at the blocked side. This is completely in agreement with the proposed conceptual plot shown in Figure 8. After finishing the crystal growth experiment inside the magnetic field, the solubility is moved back and there is mass available, but the orientation of the lysozyme molecules in the solvent, produced again the formation of monoclinic submicrometer crystallites that are sedimented on the surface and not grow-in and develop into larger sized crystals as heterogeneous nucleation.

4. Conclusions

We have studied the effect of space group on crystal orientation by testing different space groups as well as the content of alpha-helices. Thaumatin tetragonal $P4_12_12$ (rich in β-sheets) was also important to be analyzed. Besides its high beta-sheet secondary structure content, even it was oriented in the presence of the strong magnetic field. The content of α-helix is, in general, important in terms of the anisotropy of the diamagnetic susceptibility of the peptide bond used to orient these crystals (as shown for lysozyme, INHA-NAD), but sometimes it is limited by the crystallographic symmetry as shown for ferritin (cubic system) and so are the solubility changes inside the magnetic field (lysozyme tetragonal and monoclinic). The polarity of the space group, as shown for the monoclinic lysozyme, played an important role in these investigations into crystal growth behavior in the presence of a strong magnetic field.

The changes in the crystallization behavior, crystal orientation, crystal quality, and crystal morphology investigated in this contribution, using a strong magnetic field, permits one to understand how this magnetic field affects the crystal growth in batch crystallization conditions (separating the nucleation and crystal-growth processes), where it is usually a self-organized process. It has been observed that gel-growth in magnetic field, using diluted concentrations of agar, is not necessary to grow high-quality crystals; solution-growth is enough. However, diluted agar regulates the crystal size and allows removing the crystals easily from the capillary tube. It is important to remark that in order to improve the crystal quality by means of using magnetic fields, the agar should be mostly used in higher concentrations; for instance, 0.2% (w/v) was a suitable one, although the orientation could be affected due to the strength of the gel's concentration.

The crystal quality enhancement of the protein crystals grown in the presence of a strong magnetic field, observed at higher concentrations of gel, is probably a combination of the transport control imposed by the gel-growth (reducing the fluctuations amplitude of the defects in the crystal network) as well as the kinetic surface control because of the magnetic field. Finally, the increase of crystal quality is obtained when the concentration of the gel is higher (0.2% w/v) and when the intensity of the magnetic field is very high. The only disadvantage of this proposal is that the knowledge about the batch crystallization conditions is necessary to implement this strategy of crystal growth for the novo proteins.

Acknowledgment. One of the authors (A.M.) acknowledges financial support for a sabbatical year in the University of Cambridge from CONACYT project No. 91999 and DGAPA-UNAM for the traveling expenses. All authors acknowledge to Dr. Carlo Petosa for the support during X-ray data collection beamline ID14-4 at ESRF, also to the support staff of beamline I03 from the Diamond Light Source (Didcot, UK), the support staff of the beamline PXIII at the Swiss Light Source (SLS), and to Prof. Sir Tom L. Blundell for stimulating discussions and suggestions. Sachin Surade acknowledges the financial support from the European Union Sixth Framework Programme NM4TB. T.O. was supported by Overseas Research Studentship (ORS). We fully appreciate the supply of two model proteins to complete this research and data collection in Grenoble (France) from Dr. Victor M.

Bolanos-Garcia. One of the authors (A.M.) acknowledges Dr. Lynn Sibanda for the support of one of the experiments that was inside the NMR magnetic field of 11.75 T for 7 days.

References

(1) Boistelle, R.; Astier, J. P. *J. Cryst. Growth* **1988**, *90*, 14–30.
(2) Chernov, A. A. *Modern Crystallography III: Crystal Growth*; Springer: Berlin, 1984.
(3) Sarig, S. *Handbook of Crystal Growth*; Hurle, D. T. J., Ed.; North-Holland: Amsterdam, 1994; Vol 2B.
(4) Bennema, P. *J. Cryst. Growth* **1974**, *24*, 76–83.
(5) Hurle, D. T. J. *Handbook of Crystal Growth*; North-Holland: Amsterdam, 1994; Vol 1B.
(6) Gutiérrez-Quezada, A. E.; Arreguín-Espinosa, R.; Moreno, A. *Handbook of Crystal Growth*; Springer: Berlin, 2009; Vol. 1, Chapter 47.
(7) Rosenberger, F. *J. Cryst. Growth* **1986**, *76*, 618–636.
(8) Cheng, P. S.; Shlichta, P. J.; Wilcox, W. R.; Lefever, R. A. *J. Cryst. Growth* **1979**, *47*, 43–60.
(9) Petrova, E.; Dold, P.; Tsukamoto, K. *J. Cryst. Growth* **2007**, *304*, 141–149.
(10) McPherson, A. *Crystallogr. Rev.* **1996**, *6*, 157–308.
(11) Rosenberger, F. *Fundamentals of Crystal Growth I, Macroscopic Equilibrium Concepts*; Springer: Berlin, 1979.
(12) Wakayama, N. I.; Ataka, M.; Abe, H. *J. Cryst. Growth* **1997**, *178*, 653–656.
(13) Qi, J.; Wakayama, N. I.; Ataka, M. *J. Cryst. Growth* **2001**, *232*, 132–137.
(14) Lin, S. -X.; Zhou, M.; Azzi, A.; Xu, G. -J.; Wakayama, N. I.; Ataka, M. *Biochem. Biophys. Res. Commun.* **2000**, *275*, 274–278.
(15) Sato, T.; Yamada, Y.; Saijo, S.; Hori, T.; Hirose, R.; Tanaka, N.; Sazaki, G.; Nakajima, K.; Igarashi, N.; Tanaka, M.; Matsuura, Y. *Acta Crystallogr.* **2000**, *D56*, 1079–1083.
(16) Zhong, C.; Wakayama, N. I. *J. Cryst. Growth* **2001**, *226*, 327–332.
(17) Wang, L.; Zhong, C.; Wakayama, N. I. *J. Cryst. Growth* **2002**, *237*, 312–316.
(18) Yin, D. C.; Wakayama, N. I.; Inatomi, Y.; Huang, W. D.; Kuribayashi, K. *Adv. Space Res.* **2003**, *32*, 217–223.
(19) Lübbert, D.; Meents, A.; Weckert, E. *Acta Crystallogr.* **2004**, *D60*, 987–998.
(20) Qi, J.; Wakayama, N. I. *Phys. Fluids* **2004**, *16*, 3450–3459.
(21) Moreno, A.; Quiroz-García, B.; Yokaichiya, F.; Stojanoff, V.; Rudolph, P. *Cryst. Res. Technol.* **2007**, *42*, 231–236.
(22) Gavira, J. A.; García-Ruiz, J. M. *Cryst. Growth Des.* **2009**, *9*, 2610–2615.
(23) Astier, J. P.; Veesler, S.; Boistelle, R. *Acta Crystallogr.* **1998**, *D54*, 703–706.
(24) Sakurazawa, S.; Kubota, T.; Ataka, M. *J. Cryst. Growth* **1999**, *196*, 325–331.
(25) Otwinowski, Z.; Minor, W. In *Methods in Enzymology*; Carter, C. W., Sweet, R. M., Eds.; *Macromolecular Crystallography* Part A; Academic Press: New York, 1997; Vol. 276, pp 307−326.
(26) Sazaki, G.; Moreno, A.; Nakajima, K. *J. Cryst. Growth* **2004**, *262*, 499–502.
(27) Davey, R. J. *J. Cryst. Growth* **1986**, *76*, 637–644.
(28) Mikol, V.; Hirsch, E.; Giegé, R. *J. Mol. Biol.* **1990**, *213*, 187–195.
(29) Wilson, W. W. *J. Struct. Biol.* **2003**, *142*, 56–65.
(30) Astier, J. P.; Veesler, S. *Cryst. Growth Des.* **2008**, *8*, 4215–4219.
(31) Moreno, A.; Yokaichiya, F.; Dimasi, E.; Stojanoff, V. *Ann. N.Y. Acad. Sci.* **2009**, *1161*, 429–436.
(32) Vekilov, P. G.; Iwan, J.; Alexander, D.; Rosenberger, F. *Phys. Rev. Lett.* **1996**, *E54*, 6650–6660.
(33) Durbin, S. D.; Feher, G. *J. Cryst. Growth* **1991**, *110*, 41–51.
(34) Grimbergen, R. F. P.; Boek, E. S.; Meekes, H.; Bennema, P. *J. Cryst. Growth* **1999**, *207*, 112–121.
(35) Heijna, M. C. R.; van Enckevort, W. J. P.; Vlieg, E. *Cryst. Growth Des.* **2008**, *8*, 270–274.
(36) Hondoh, H.; Sazaki, G.; Miyashita, S.; Durbin, S. D.; Nakajima, K.; Matsuura, Y. *Cryst. Growth Des.* **2001**, *1*, 327–332.
(37) Matsuura, Y.; Chernov, A. A. *Acta Crystallogr.* **2003**, *D59*, 1347–1356.